ResearchGate

See discussions, stats, and author profiles for this publication at: https://www.researchgate.net/publication/234956624

Analysis of the sign reversal of the second-order molecular polarizability in polymethineimine chains

ARTICLE *in* THE JOURNAL OF CHEMICAL PHYSICS · OCTOBER 2001

Impact Factor: 2.95 · DOI: 10.1063/1.1401822

CITATIONS
21

READS
24

6 AUTHORS, INCLUDING:

Denis Jacquemin
University of Nantes
356 PUBLICATIONS **8,265** CITATIONS
SEE PROFILE

David Beljonne
Université de Mons
355 PUBLICATIONS **15,289** CITATIONS
SEE PROFILE

Victor Geskin
Université de Mons
75 PUBLICATIONS **1,781** CITATIONS
SEE PROFILE

Jean-Marie André
University of Namur
280 PUBLICATIONS **5,922** CITATIONS
SEE PROFILE

Available from: Denis Jacquemin
Retrieved on: 25 January 2016

Analysis of the sign reversal of the second-order molecular polarizability in polymethineimine chains

Denis Jacquemin[a)]
Laboratoire de Chimie Théorique Appliquée, Facultés Universitaires Notre-Dame de la Paix, rue de Bruxelles, 61, B-5000 Namur, Belgium

David Beljonne[b)]
Centre de Recherche en Electronique et Photonique Moléculaires, Service de Chimie des Matériaux Nouveaux, Université de Mons-Hainaut, B-7000 Mons, Belgium and Department of Chemistry, The University of Arizona, Tucson, Arizona 85721-0041

Benoît Champagne[c)]
Laboratoire de Chimie Théorique Appliquée, Facultés Universitaires Notre-Dame de la Paix, rue de Bruxelles, 61, B-5000 Namur, Belgium

Victor Geskin
Centre de Recherche en Electronique et Photonique Moléculaires, Service de Chimie des Matériaux Nouveaux, Université de Mons-Hainaut, B-7000 Mons, Belgium

Jean-Luc Brédas
Centre de Recherche en Electronique et Photonique Moléculaires, Service de Chimie des Matériaux Nouveaux, Université de Mons-Hainaut, B-7000 Mons, Belgium and Department of Chemistry, The University of Arizona, Tucson, Arizona 85721-0041

Jean-Marie André
Laboratoire de Chimie Théorique Appliquée, Facultés Universitaires Notre-Dame de la Paix, rue de Bruxelles, 61, B-5000 Namur, Belgium and Department of Chemistry, The University of Arizona, Tucson, Arizona 85721-0041

(Received 12 April 2001; accepted 18 July 2001)

The second-order polarizability tensor (β) components of polymethineimine oligomers have been computed with the semiempirical intermediate neglect of differential overlap (INDO) coupled either to sum-over-states (SOS) or finite-field real space approach. Our goal is to rationalize the sign reversal of the longitudinal β component with chain length. The INDO results are shown to compare well with the values obtained from previous *ab initio* calculations. Using a four-state SOS model that reproduces correctly the evolution of β with chain length, we demonstrate that the shape of the β curve can be explained as resulting from the competition between two contributions of opposite signs. In the framework of a real-space approach, those contributions are found to correspond to bond charge and bond polarization phenomena. © *2001 American Institute of Physics.*
[DOI: 10.1063/1.1401822]

I. INTRODUCTION

Since its synthesis by Wöhrle some 25 years ago[1,2] polymethineimine (PMI, also named polycarbonitrile or polynitrile, Fig. 1), $(CH{=}N)_N$, has been the focus of several theoretical studies. Three main topics have been addressed: (i) The band structure of PMI has been computed at the extended Hückel,[3] valence effective Hamiltonian,[4] modified neglect of diatomic overlap,[5] *ab initio* Hartree-Fock (HF),[6–8] density functional theory (DFT),[9–11] and second-order Møller-Plesset (MP2)[12] levels. (ii) Geometry optimizations have been carried out with the HF,[6,13,14] DFT,[9–11] and MP2[12] techniques; the results show that, as in polyacetylene (PA), the bond-length alternating structure is the most stable. (iii) The nonlinear optical (NLO) properties have been evaluated with a wide range of methodologies on short[15–19] and long[20–24] oligomers as well as on the polymer[25–27] in order to evaluate the magnitude of the second-order polarizability (β). The longitudinal component of the β tensor (β_{xxx} with x the longitudinal axis) of PMI oligomers scaled to its molecular weight is very large compared to that of classical push-pull molecules.[24] The analysis of the evolution with chain length of β_{xxx} and the understanding of the origin of the β response of PMI are thus of interest in the search for new kinds of NLO materials.

The ground-state longitudinal dipole moment of PMI oligomers is directed from the N-end towards the C-end of the molecule; its sign is positive for all oligomers and independent of the molecular size. Hereafter, the sign of β_{xxx} is taken as positive when $\beta_{xxx}\uparrow\uparrow\mu_x$ (or negative when $\beta_{xxx}\uparrow\downarrow\mu_x$), which is consistent with the convention that the sign of β_{xxx} is the same as the sign of the projection of β_{xxx} on μ_x. Coupled Hartree–Fock (CHF) calculations on all-

[a)]Post-doctoral Researcher of the Belgian National Fund for Scientific Research.
[b)]Research Associate of the Belgian National Fund for Scientific Research.
[c)]Senior Research Associate of the Belgian National Fund for Scientific Research.

 © 2001 American Institute of Physics

Downloaded 24 Sep 2003 to 138.48.16.177. Redistribution subject to AIP license or copyright, see http://ojps.aip.org/jcpo/jcpcr.jsp

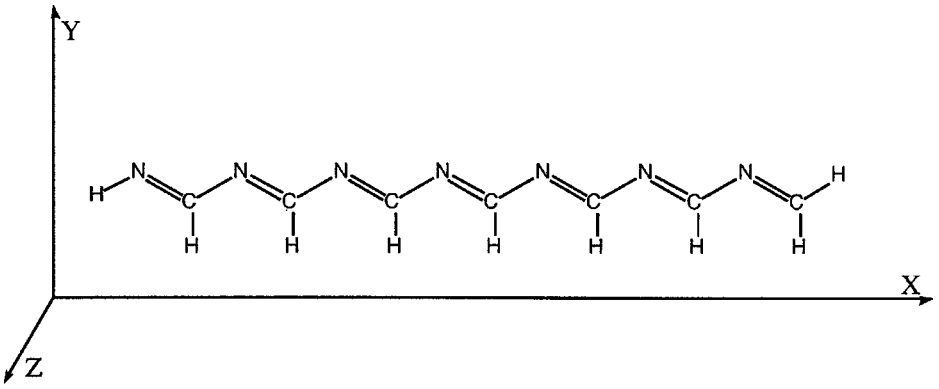

FIG. 1. Orientation of polymethine-imine oligomers in the Cartesian frame.

trans conformers indicate a remarkable characteristic: β_{xxx} is seen to reverse sign as a function of increasing chain length, N. The β_{xxx}/N [as well as $\Delta\beta_{xxx}(N)=\beta_{xxx}(N)-\beta_{xxx}(N-1)$] value starts negative, reaches a negative peak, then turns positive, and slowly tends to an asymptotic positive value (see Fig. 2).[21–24]

Our goal here is therefore to analyze and rationalize the evolution of $\beta_{xxx}(N)/N$ and in particular the sign change in $\beta_{xxx}(N)$. Our analysis is based on the complementary pictures provided by the SOS and FF methods.

In a previous work carried out at the Pariser–Parr–Pople (PPP) level,[21] the SOS scheme had been used within the uncoupled Hartree–Fock (UCHF) approach to evaluate $\beta_{xxx}(N)$ and rationalize its chain-length dependence in terms of the most significant excited states.[21] However, since the UCHF scheme neglects the electron-hole interaction, the UCHF and CHF $\beta_{xxx}(N)$ evolutions present different long-chain behaviors. Thus, in the present work, we have chosen the INDO/SCI formalism, that includes part of the electron-hole correlation, in order to carefully address the chain-length dependence of $\beta_{xxx}(N)$. The INDO/SCI method is found to reproduce adequately the *ab initio* CHF behavior even when a restricted set of excited states (and/or channels) is taken into account; in addition, it provides an easy analysis of the excitations at the origin of the second-order hyperpolarizability.[28,29]

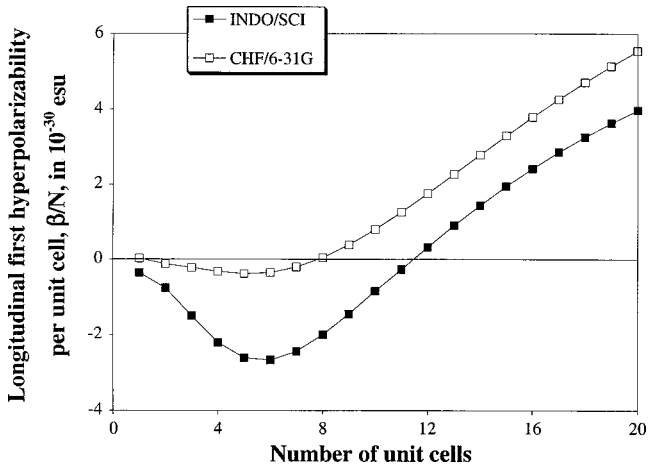

FIG. 2. Evolution of $\beta_{xxx}(N)/N$ with oligomer length at the CHF/6-31G and INDO/SCI levels. All results are in 10^{-30} esu (to convert to a.u., multiply by 115.7).

A second picture is also used, based on the analysis of the field-induced changes in dipole moment and of its derivatives due to the local polarizations of the atoms and bonds. This gives a different interpretative scheme for the static molecular polarizabilities. Here this analysis is performed within a FF approach coupled to INDO/HF estimates of the Mulliken charges. This approach was successful to rationalize the cubic polarizability of various conjugated systems.[30–32]

II. METHODOLOGY

A. Geometry optimization

Geometry optimizations on all-*trans* PMI oligomers have been carried out at the RHF/6-31G level using the GAUSSIAN94 package;[33] the residual forces at the end of the optimization were limited to 10^{-5} a.u. The orientation of the chains (see Fig. 1) is such that x is the longitudinal direction, y is the transverse direction and defines with x the σ plane. z is the perpendicular one (i.e., the plane of the π electrons). Note that geometry optimizations result in slightly curved backbones since the valence angles around carbons and nitrogens differ by some 2 degrees. The choice of the longitudinal axis is therefore not totally rigorous. However, for the chain lengths considered in this work (up to 20 CN units), it does not affect the longitudinal β_{xxx} values in any appreciable way.

The geometrical parameters obtained for the longest oligomer studied ($N=20$) are compared in Table I to the infinite-chain limits obtained by Hirata[11] and Sun[12] who assumed linearity of the polymers. Our results are in perfect agreement with those of Sun[12] computed at the same level of theory (RHF/6-31G) indicating that the longest oligomer has a converged geometry. In the conjugated system, the most significant structural parameter is the degree of bond-length alternation (BLA$=d_{C=N}-d_{N-C}$). The RHF/6-31G BLA of 0.117 Å is, as expected, larger than the BLA evaluated by using electron correlated methods [0.073 (0.085) Å at the B3LYP/3-21G (MP2/6-31G**) levels]. Bond angles are rather insensitive to the method of computation (variations smaller than 2 degrees). For a more complete discussion of

Downloaded 24 Sep 2003 to 138.48.16.177. Redistribution subject to AIP license or copyright, see http://ojps.aip.org/jcpo/jcpcr.jsp

TABLE I. Geometry of PMI obtained by different *ab initio* methods. The bond lengths (d) are in Å, the bond angles (α) in degrees.

Method	$d_{C=N}$	d_{N-C}	d_{C-H}	$\alpha_{C=N-C}$	$\alpha_{N-C=N}$	$\alpha_{N=C-H}$	Ref.
RHF/6-31G	1.268	1.385	1.089	119.2	121.1	121.6	This work
RHF/6-31G	1.267	1.384	1.088	120.3	120.3	121.8	12
B3LYP/3-21G	1.300	1.373	1.108	119.0	119.0	121.9	11
MP2/6-31G**	1.286	1.371	1.102	118.2	118.2	122.2	12

the electron correlation and basis set effects, we refer the reader to Ref. 12.

B. Calculation of the second-order polarizability

The changes in energy E and dipole moment $\vec{\mu}$ of a molecular system due to the reorganization of its charge distribution under the application of a static uniform electric field $\vec{F}$, is traditionally expanded in a Taylor series:

$$E = E_0 - \frac{1}{1!}\vec{\mu_0}.\vec{F} - \frac{1}{2!}\vec{\alpha}:\vec{F}\vec{F} - \frac{1}{3!}\vec{\vec{\beta}}:\vec{F}\vec{F}\vec{F} - \frac{1}{4!}\vec{\vec{\vec{\gamma}}}:\vec{F}\vec{F}\vec{F}\vec{F} - \cdots, \quad (1)$$

$$\vec{\mu} = \vec{\mu_0} + \frac{1}{1!}\vec{\alpha}.\vec{F} + \frac{1}{2!}\vec{\vec{\beta}}:\vec{F}\vec{F} + \frac{1}{3!}\vec{\vec{\vec{\gamma}}}:\vec{F}\vec{F}\vec{F} + \cdots, \quad (2)$$

where $\vec{\alpha}$ is the (electric dipole) static linear polarizability tensor; $\vec{\vec{\beta}}$ and $\vec{\vec{\vec{\gamma}}}$ are the static second- and third-order polarizability tensors. In our study, the chain geometries are kept frozen. Thus, only the electronic component of the β tensor is evaluated and no vibrational effects are considered. The value of β per unit cell

$$\frac{\beta(N)}{N} \quad (3)$$

is taken as a good figure of merit for the efficiency of the second-order nonlinear response.

1. INDO/SCI approach

In the INDO/SCI computational scheme, the singlet excited states that define the many-electron basis for the SOS perturbational expansion are obtained by the semiempirical INDO[34] method. Here, all π orbitals are included in the CI active space and the resulting excited-state wave functions are plugged into the SOS expression for $\beta(N)$,[35]

$$\vec{\vec{\beta}} = 6\sum_j \sum_k \frac{\langle\Psi_0|\vec{\mu}|\Psi_j\rangle\overline{\langle\Psi_j|\vec{\mu}|\Psi_k\rangle}\langle\Psi_k|\vec{\mu}|\Psi_0\rangle}{(E_0 - E_j)(E_0 - E_k)}, \quad (4)$$

Ψ_0 is the ground state wave function of energy E_0, Ψ_j is the jth excited state of energy E_j, $\vec{\mu}$ is the dipole moment operator and

$$\overline{\langle\Psi_j|\vec{\mu}|\Psi_k\rangle} = \langle\Psi_j|\vec{\mu}|\Psi_k\rangle - \langle\Psi_0|\vec{\mu}|\Psi_0\rangle\delta_{jk}. \quad (5)$$

Since all singlet π excited states are included in the SOS procedure, fully converged and size-consistent SCI $\beta(N)$ values are obtained.

2. Real-space approach

The real-space approach to molecular (hyper)polarizability is inspired by the ideas formulated by Chopra *et al.*[36] and Nakano *et al.*[37] It is based on the analysis of the field-induced electron density shifts that lead to the changes of the dipole moment. Applied in this work to the second-order polarizability, this approach is basically similar to that used by us previously to rationalize the third-order polarizability of conjugated systems.[30–32]

The dipole moment is the moment of both the positive nuclear charges Q_i and the negatively charged electron density. Since Mulliken, it has become common to partition the electron density into ''atomic'' charges q_i:

$$\mu_x \approx \sum_i x_i(Q_i + q_i). \quad (6)$$

Since the nuclear charges Q_i are constant and we do not include any vibrational effects, all nuclear displacements are neglected and thus the atomic coordinates x_i are independent of **F**. The longitudinal component of the static quadratic polarizability β_{xxx} then writes

$$\beta_{xxx} = \left(\frac{\partial^2\mu_x}{\partial F^2}\right)\Bigg|_{F=0} \approx \sum_i x_i\left(\frac{\partial^2 q_i}{\partial F^2}\right)\Bigg|_{F=0} \equiv \sum_i x_i q_i^{(2)}. \quad (7)$$

In such a real-space approach, β_{xxx} is partitioned into local contributions $x_i q_i^{(2)}$, the so-called *β-moments* based on *β-charges* $q_i^{(2)}$.

The local atomic contributions can be further condensed by collecting the β-charges into pairs of neighboring atoms p:

$$b_p^+ \equiv q_{2p}^{(2)} + q_{2p-1}^{(2)} = (q_{2p} + q_{2p-1})^{(2)}, \quad (8)$$

$$b_p^- \equiv q_{2p}^{(2)} - q_{2p-1}^{(2)} = (q_{2p} - q_{2p-1})^{(2)}, \quad (9)$$

and defining corresponding ''condensed'' coordinates:

$$x_p^+ \equiv \frac{(x_{2p} + x_{2p-1})}{2}, \quad (10)$$

$$x_p^- \equiv \frac{(x_{2p} - x_{2p-1})}{2}. \quad (11)$$

It is straightforward to express β_{xxx} via these quantities:

$$\sum_i x_i q_i^{(2)} = \sum_p b_p^+ x_p^+ + \sum_p b_p^- x_p^- \equiv \beta^+ + \beta^-, \quad (12)$$

where the summation runs over all the pairs of atoms. For a π-conjugated chain, it is convenient to choose the pairs in such a way that they involve atoms linked via a double bond, i.e., the C=N bond in the present PMI study.

Downloaded 24 Sep 2003 to 138.48.16.177. Redistribution subject to AIP license or copyright, see http://ojps.aip.org/jcpo/jcpcr.jsp

Each pair of the so-defined elements has now the simple meaning:

(i) x_p^+ is the longitudinal coordinate of the double bond center, roughly linear in p and varying in the range of molecular length;

(ii) x_p^- is the half-length of the longitudinal projection of the double bond, roughly constant in p (ca. 0.5 Å);

(iii) b_p^+ is the second derivative of the sum of the charges on the atoms forming the selected bond. It reflects the nonlinear polarization of a double bond seen as a whole entity due to the field-induced charge transfer from the rest of the molecule; the terms b_p^+ and $b_p^+ x_p^+$ correspond to *bond charge nonlinearities*;

(iv) b_p^- is the second derivative of the difference of the charges on the atoms of the bond (bond polarity). It reflects its internal nonlinear polarization; the terms b_p^- and $b_p^- x_p^-$ correspond to *bond polarization nonlinearities*.

It is straightforward to prove that the sum of the (hyper)polarizability charges, at any order m, is zero by virtue of electric charge conservation:

$$\sum_i q_i^{(m)} = \frac{\partial^m \left(\sum_i q_i \right)}{\partial F^m} = 0. \tag{13}$$

The same property holds for the sum of all b_p^+. Note also that, as is usual in moment theory, each local moment depends on the (arbitrary) choice of the coordinate origin. Nevertheless, the sum of all β-moments yielding β_{xxx}, or of its partitioned moments, β^+ and β^-, is invariant. All the quantities related to the β-moments $q_x^{(2)}$ change sign upon x axis inversion; since μ_x also changes sign, the sign of the projection of β_{xxx} on μ_x remains unaltered.

In our study, the β-charges have been calculated from the INDO/HF Mulliken charges. The FF expansion of the charges has been limited to the second power of **F**; the maximum electric field applied is 0.002 a.u. ($1.028\,44 \times 10^7$ V/cm).

III. RESULTS

INDO/SCI test calculations on the seven shortest oligomers were carried out including all valence (π and σ) electrons; the results show that the π electrons are responsible for most of the nonlinear response. From the comparison between previous PPP and all-electron *ab initio* investigations,[21,22] it can be concluded that the inclusion of σ electrons in the calculation leads to a small increase of the value of β and displaces slightly the position (by one or two unit cells) of its maximum towards larger chain size in the $\beta_{xxx}(N)$ curve; however, it does not influence the shape of the β_{xxx}/N curve.

Figure 2 compares our INDO/SCI results with those from *ab initio* CHF/6-31G calculations (Ref. 24). Although the absolute value of the extremum is larger at the INDO/SCI level, the shapes of the two β_{xxx}/N curves are similar. The oligomer lengths corresponding to the negative peak differ only by one unit cell, the positions of the sign change by two, and the saturation takes place for similar chain lengths.

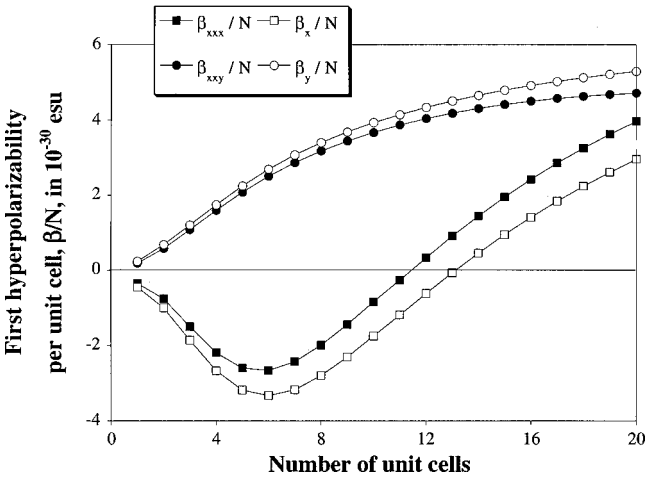

FIG. 3. Evolution with oligomer length of INDO/SCI β_{xxx}/N, β_x/N, β_{xxy}/N, and β_y/N. Values are in 10^{-30} esu.

The INDO/SCI $\beta(N)/N$ evolutions are sketched in Fig. 3 for two different tensor and vector components of β. It is clear from the figure that β_x and β_y [due to the planar symmetry of PMI, β_x and β_y are computed as $\beta_x = \beta_{xxx} + \frac{1}{3}(\beta_{xyy} + \beta_{xzz} + 2\beta_{yyx} + 2\beta_{zzx}) = \beta_{xxx} + \beta_{xyy}$, $\beta_y = \beta_{yyy} + \frac{1}{3}(\beta_{yxx} + \beta_{yzz} + 2\beta_{xxy} + 2\beta_{zzy}) = \beta_{yyy} + \beta_{xxy}$ in the INDO/SCI framework] mainly originate from β_{xxx} and β_{xxy}, respectively. The longitudinal component follows the behavior described in the introduction while the β_y evolution is more traditional with its direct saturation pattern. It is also interesting to note that, for short chains, β_x/N and β_y/N are of the same order of magnitude: $|\beta_x|$ is nearly the same as $|\beta_y|$ for $N=7$, vanishes for $N=13$ (i.e., when β_x/N passes by zero), and approximately reaches one half $|\beta_y|$ for $N=19$.

A. Second-order polarizability of polymethineimine oligomers via SOS analysis

In order to analyze more easily the evolution of the β_{xxx}/N curve, the full INDO/SCI approach has been restricted to a limited set of channels and excited states. Figure 4 gives the evolution of β_{xxx} as a function of the number of excited states included in the SOS approach for three oligomers of size $N=8$, 12, and 20. The number of excited states that significantly contribute to β_{xxx} grows with N; however, for small and medium chains, only a limited number of states dominates the nonlinear response. We have therefore examined more closely the results obtained by considering models of increasing complexity (two-state, three-state, four-state, etc., models). Within such schemes, the total β_{xxx} response can be formally decomposed into two types of excitation channels: dipolar-type terms

$$0 \rightarrow m \rightarrow m \rightarrow 0 \tag{14}$$

and crossed, two-photon-like terms

$$0 \rightarrow m \rightarrow n \rightarrow 0. \tag{15}$$

In these equations, 0 corresponds to the ground state, m and n to excited states. The arrows represent transition moments

Downloaded 24 Sep 2003 to 138.48.16.177. Redistribution subject to AIP license or copyright, see http://ojps.aip.org/jcpo/jcpcr.jsp

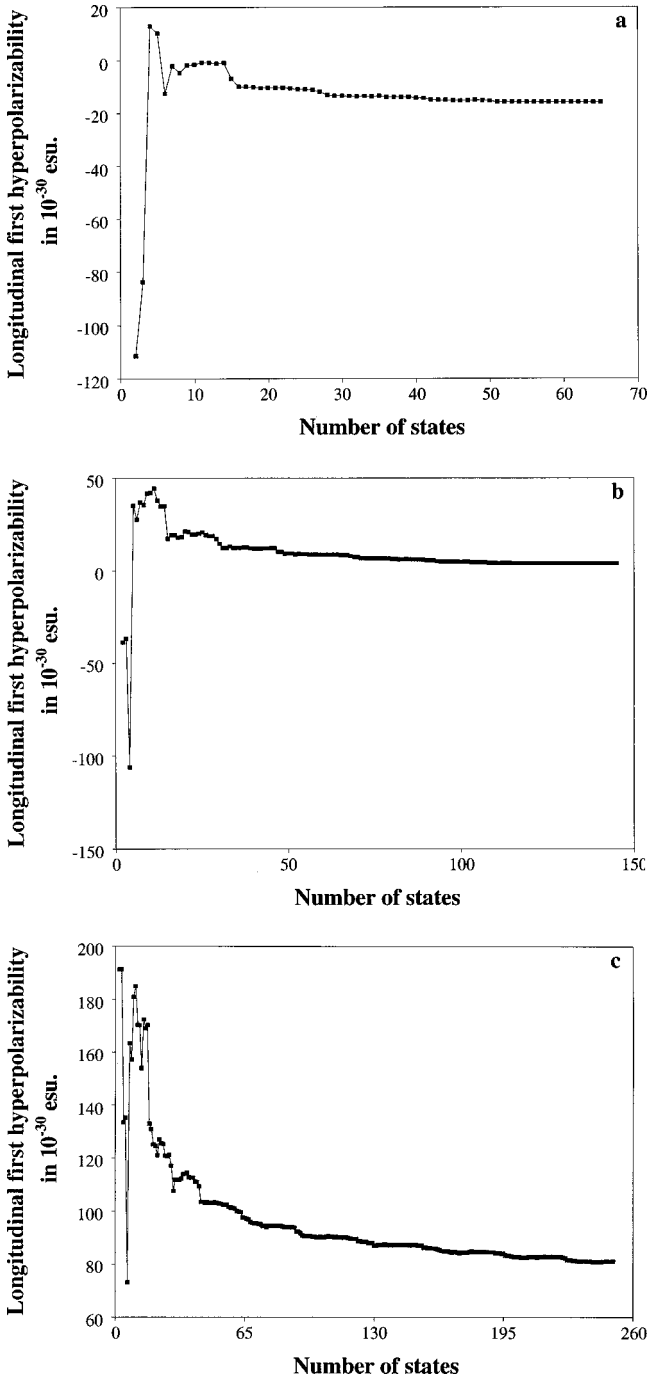

FIG. 4. Evolution of β_{xxx} as a function of the number of INDO/SCI states taken into account in the SOS approach. The (a), (b), and (c) graphs correspond to $N=8$, $N=12$, and $N=20$, respectively.

when $m \neq n$, or differences between the excited-state and ground-state dipole moments when $m=n$. For example, the dipolar term of the two-state model restricted to the lowest excited state, $m=1$, reads

$$\beta = 6 \frac{(\mu_{01})^2[\mu_{11}-\mu_{00}]}{(E_{01})^2} \tag{16}$$

with E_{01} the transition energy between the ground and first excited state.

The dipolar and two-photon contributions [from Eqs. (14) and (15)] are illustrated in Fig. 5. The so-called total

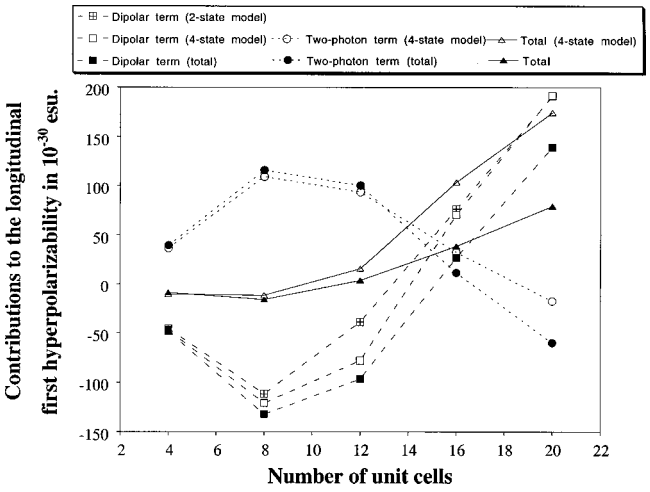

FIG. 5. Contributions to β_{xxx} in the various models. The squares correspond to the results of Eq. (14), the circles to Eq. (15) and the triangles to the total.

values are those calculated by considering all dipolar and two-photon terms; we present the results of the two-state model and of a four-state model which, in addition to states 0 and 1 of the two-state model, also includes two higher lying states, referred to as states 2 and 3 in the following. Within the four-state model, the β response is obtained by summing the dipolar terms (14) with $m=1$, 2, and 3 and the two-photon terms (15) with $m=1$ and $n=2,3$. Figure 5 shows that, for small chains ($\sim N<10$), the four-state model is a good approximation and reproduces the chain-length dependence of β_{xxx} as provided by the total SOS expansion. For longer oligomers, the agreement becomes gradually poorer since a larger number of excited states comes into play in the SOS expansion. Obviously, the formalism then loses its simplicity as a means to understand the origin of the NLO response curve.

The limited SOS second-order response of PMI chains is seen to result from the cancellation of large contributions of opposite signs; such an interplay between the dipolar terms and their two-photon counterparts of opposite sign has already been found in push–pull systems.[38] However, it is striking to observe that both dipolar and two-photon sums change sign as N increases. The detailed analysis of this feature is given below.

As seen in Fig. 5, the two-state model, which does not take any two-photon-type channels into account strongly overestimates β_{xxx} and the maximum absolute value. However, it reproduces well both the positions of the negative extremum and of the sign reversal. This contrasts with the UCHF/PPP study where the two-state model gives results in total disagreement with the CHF values. Figure 6 displays the various terms of Eq. (16). The excitation energy E_{01} decreases slowly with increasing chain length while the transition dipole moment μ_{01} increases continuously with N. A fitting procedure shows that, for large N, μ_{01} presents a $N^{1/2}$ behavior ($R=0.9998$), as expected from an analysis of the two-state model applied to the linear polarizability α. (In the two-state model, the linear polarizability is the the ratio between the squared transition moment and the excitation energy; in long chains, the excitation energy is nearly constant

Downloaded 24 Sep 2003 to 138.48.16.177. Redistribution subject to AIP license or copyright, see http://ojps.aip.org/jcpo/jcpcr.jsp

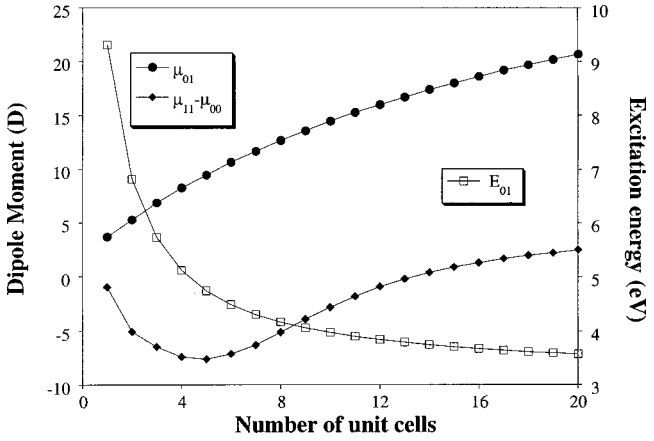

FIG. 6. Evolution with chain length of the parameters entering the β_{xxx} expression in the two-state model Eq. (16).

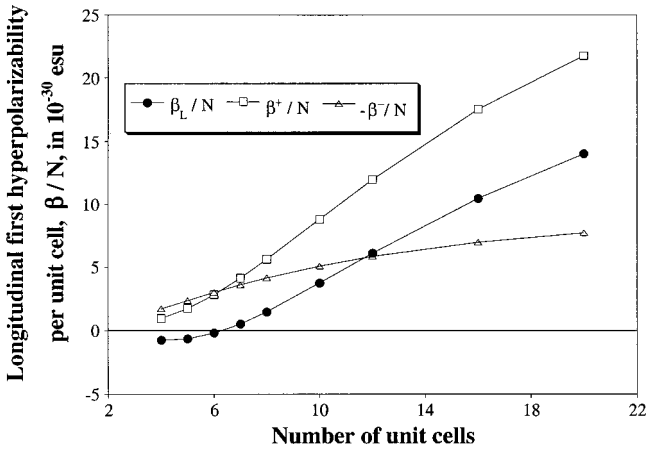

FIG. 8. Evolution with oligomer length of $\beta_{xxx}(N)/N$ as obtained from INDO/HF π-electron β-moments and its bond charge (β^{+}/N) and bond polarization (β^{-}/N) components. All results are in 10^{-30} esu.

while the polarizability is proportional to the size of the molecule; the transition dipole moment is thus predicted to evolve as $N^{1/2}$.)

The $[\mu_{11}-\mu_{00}]$ term presents the same shape as β_{xxx}, shape, i.e., a negative maximum ($N=5$) and a sign change ($N=14$). The evolution of μ_{00} and μ_{11} is given in Fig. 7: μ_{00} is always positive and monotonously increases with chain length while μ_{11} is initially negative, reaches a negative extremum, passes through zero between $N=5$ and $N=6$ and then increases more rapidly than μ_{00} (see Fig. 7). The evolution with chain length of $[\mu_{11}-\mu_{00}]$ therefore accounts for the sign reversal of the dipolar contribution to $\beta_{xxx}(N)$.

An analysis of the $n=2$ state wave function indicates that it corresponds to the so-called mA_g state, a type of state which is known to dominate the third-order nonlinear optical response of symmetric polyenes.[39] This state is strongly coupled to the first excited state (that corresponds to the $1B_u$ state of polyenes) but has a weak absorption cross section from the ground state. The contribution from channel $0\rightarrow1\rightarrow2\rightarrow0$ to the total response is positive, increases with chain length, and saturates for large oligomers. This channel provides a contribution of opposite sign with respect to the dipolar term and thus leads to a decrease of the SOS absolute β values. One can interpret this feature as arising from a retrodonation effect from the acceptor to the donor, since the state dipole moment for $n=2$ is in all cases smaller than that for $n=1$. As the chain length increases, another higher-lying excited state, $n=3$, starts to play a significant role in the description of the NLO response. This $n=3$ state has a weak coupling to state 1, but a large transition dipole moment with the ground state. It can be assimilated to a higher-lying B_u excited state of symmetric polyene chains. In contrast to channel $0\rightarrow1\rightarrow2\rightarrow0$, contribution from pathway $0\rightarrow1\rightarrow3\rightarrow0$ is always negative and becomes significant in long chains. The peaked evolution of the two-photon terms illustrated in Fig. 5 thus results from the balance between these two $0\rightarrow1\rightarrow2\rightarrow0$ and $0\rightarrow1\rightarrow3\rightarrow0$ channels.

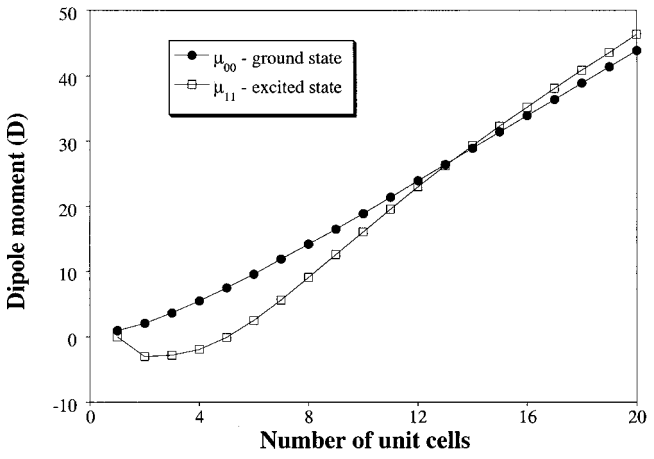

FIG. 7. Evolution of the dipole moments in the ground and lowest excited state as a function of chain length.

B. Second-order polarizability of polymethineimine oligomers via real-space analysis

The evolution of the β_{xxx}/N response as obtained from the π contributions to the β-charges of the real-space approach, is plotted in Fig. 8. The numerical values of the β_{xxx}/N response as well as the general shape with respect to chain length are in semiquantitative agreement with those obtained by the more sophisticated techniques discussed above: β_{xxx}/N is negative for short oligomers; it switches sign (at $N\sim6$), and slowly saturates in the long-chain limit.

There is no significant field-induced population transfer between the π and σ subsystems. As could be expected for π-conjugated chains, the π contributions are the most important. Even if individual σ contributions can be significant, it is seen that the sums of their β-moments (σ-hyperpolarizabilities) are (i) smaller and (ii) growing much more slowly with N than the π contributions. This justifies that the analysis of β_{xxx} be restricted to the π-electron contributions only.

The pattern of the β-charges arising from π-electron polarization of the backbone presents a lenslike envelope whose general shape is the same for all the PMI oligomers investigated. Figure 9(a) shows the atomic π-electron β-charges for $N=16$ as an example. For very long chains,

Downloaded 24 Sep 2003 to 138.48.16.177. Redistribution subject to AIP license or copyright, see http://ojps.aip.org/jcpo/jcpcr.jsp

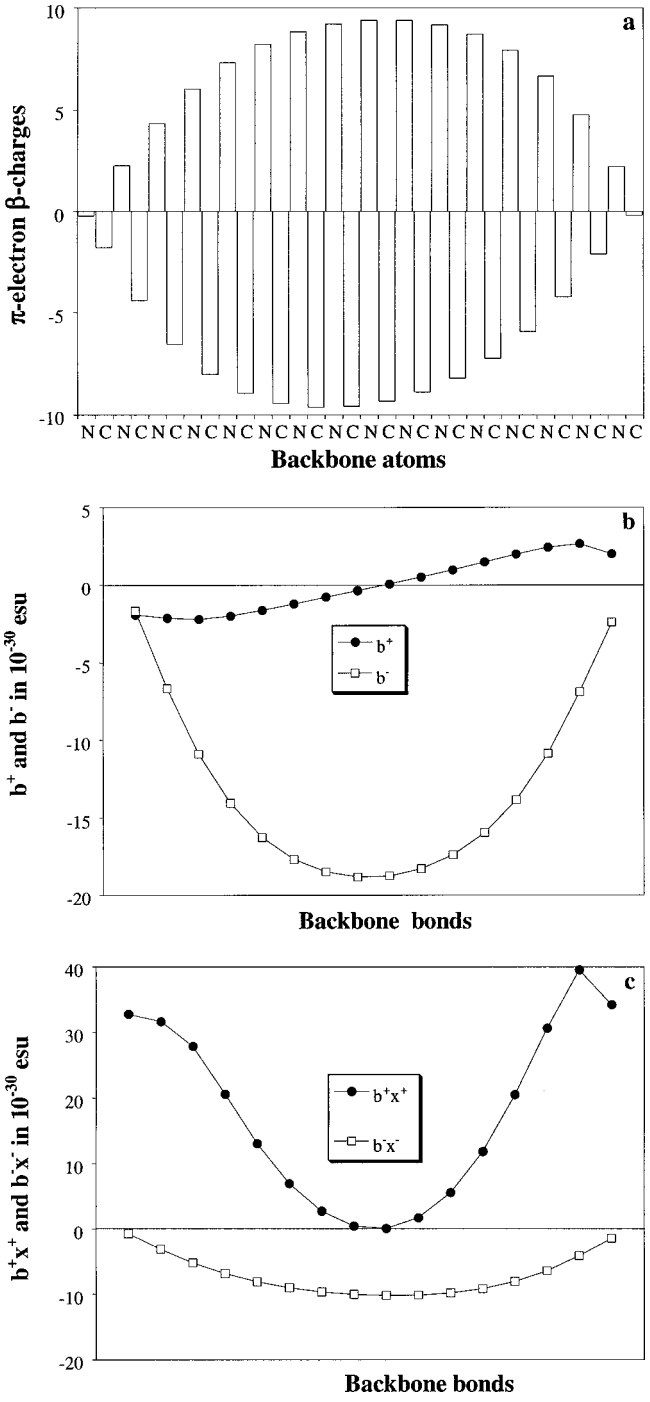

FIG. 9. β_{xxx} in the $N=16$ oligomer: (a) π-electron β-charges, (b) bond charge, b^+, and bond polarization nonlinearity, b^-, (c) bond charge and bond polarization moments, b^+x^+ and b^-x^-.

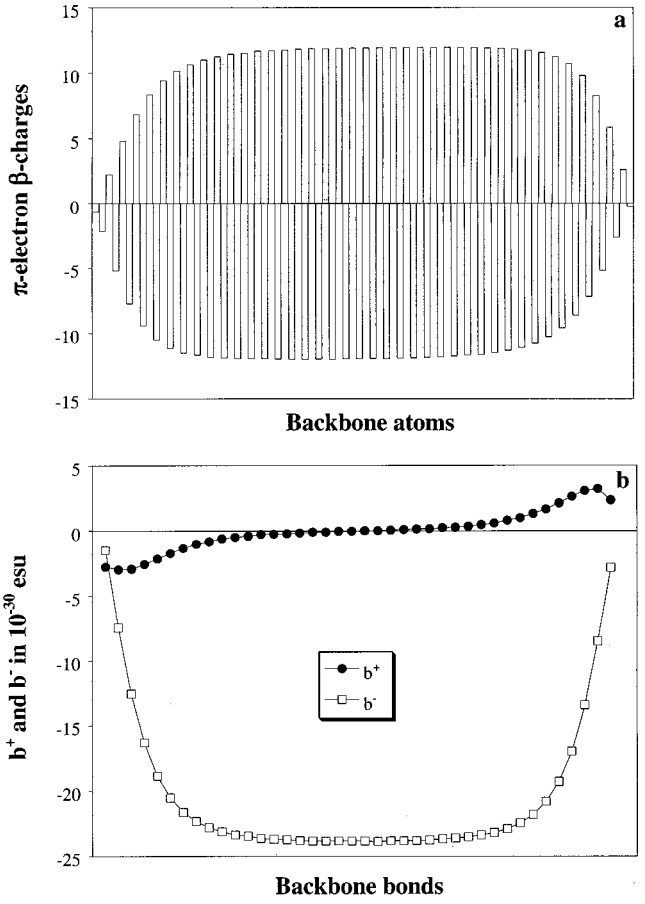

FIG. 10. β_{xxx} in the $N=40$ oligomer (linear backbone imposed): (a) π-electron β-charges, (b) bond charge, b^+, and bond polarization nonlinearity, b^-.

the envelope of the β-charges becomes rectangular in the middle, with equal responses for atoms of the same type as shown for $N=40$ in Fig. 10(a). This means that the environment of these atoms is effectively equivalent for their second-order response, i.e., the chain end effects are no longer felt after ca. 10 unit cells.

The alternating signs of $q^{(2)}$ on adjacent N and C backbone atoms apparently reflect the individual bond polarizations. We take a diatomic molecule as an example. Under the action of external static electric field the charge on one of its atoms increases while the charge of the other one decreases provided that their sum remains constant. Therefore, the field derivatives of both atomic charges, in all orders: $q^{(1)}$, $q^{(2)}$,…, are constrained to be equal in magnitude and have opposite signs. Each double C═N moiety in PMI is not exactly an isolated diatomic since its charge is not conserved under polarization. Nevertheless, these fragments retain a lot of their autonomy, as indicated by alternating sign and close values of the second derivatives of adjacent C and N atoms, i.e., their β-charges $q^{(2)}$. This alternate pattern of the β-charges suggests further that the largely compensating terms which were already noted in the perturbative SOS treatment originate from the local polarizations. Expressing atomic charges, to the second order,

$$q_C(F)=q_C(0)+q_C^{(1)}F+\tfrac{1}{2}q_C^{(2)}F^2, \tag{17}$$

$$q_N(F)=q_N(0)+q_N^{(1)}F+\tfrac{1}{2}q_N^{(2)}F^2, \tag{18}$$

we obtain for bond polarity,

$$q_C(F)-q_N(F)=[q_C(0)-q_N(0)]+[q_C^{(1)}-q_N^{(1)}]F + \tfrac{1}{2}[q_C^{(2)}-q_N^{(2)}]F^2. \tag{19}$$

As defined in Eq. (19), the bond polarity is positive at zero field and under moderate field amplitudes. Now note [Fig. 9(a)] that the sign of β-charges is positive for negatively

Downloaded 24 Sep 2003 to 138.48.16.177. Redistribution subject to AIP license or copyright, see http://ojps.aip.org/jcpo/jcpcr.jsp

charged N and negative for positively charged C (with possible exception for chain end atoms for which the magnitude is negligible). Therefore, the second-order term in Eq. (19) is negative. In this sense, one can say that, at the second order, π-electrons resist the field-induced polarization of each double bond.

Since the PMI β-charge patterns do not change qualitatively with N, an additional descriptor is needed to understand the origin of the β switching sign. In the case of PMI oligomers, this descriptor is the set of bond pair contributions introduced in Sec. II B 2.

The second-order bond polarization and bond charge nonlinearities, b^- and b^+, are shown in Figs. 9(b) ($N=16$) and 10(b) ($N=40$). The sum of the bond charge terms b^+ over all bonds is zero since the positive and negative terms that are present and grouped at opposite halves of the molecule cancel. Their signs indicate that second-order bond charge terms favor field-induced positive charge transfer towards the positively charged C-end of the molecule and negative charge transfer towards the negatively charged N-end, increasing the overall polarization of the molecule. In contrast, the negative sign of all the bond polarization terms b^- indicates that each double bond resists, at second order, the field-induced polarization, as already noted in the β-charge analysis.

To obtain the actual β values, the moments β^+ and β^- have to be evaluated according to Eq. (12). These moments are shown for $N=16$ in Fig. 9(c). All the second-order bond polarization moments b^-x^- are origin-independent and negative. The total moment β^+ is also origin independent even if its individual b^+x^+ contributions are origin dependent. If locating the x origin at the middle of the molecule, all the second-order bond charge moments b^+x^+ are positive. Thus, the invariant bond moment sums have opposite signs, $\beta^+>0$, $\beta^-<0$ for all the oligomers studied. Therefore, *it is the balance between β^+ and β^- that determines the sign and the value of β_{xxx}*. The N evolutions of β^+ and $-\beta^-$ per unit cell are illustrated in Fig. 8. The negative bond polarization contribution, β^-, prevails in short PMI molecules, while the positive bond charge contribution, β^+, becomes the dominant contribution for long chains.

The reason is the following. The highest b^-x^- polarization moments are observed in the middle of the chain since the b^- polarization bond terms are the highest in the middle as a consequence of higher atomic β-charges $q_i^{(2)}$, while the x^- values are practically constant along the chain. Furthermore, for any bond, $|b^+|$ is lower than $|b^-|$ since $q^{(2)}$ have opposite signs at carbon and nitrogen atoms. Thus $|b^+x^+|$ can only exceed $|b^-x^-|$ if $|x^+|>|x^-|$. Here, the origin of the coordinates has been located in the middle of the chain. Then, the x^+ coordinates increase towards the chain ends; therefore, the longer the chain, the higher the excess of the total $|\beta^+|$ moment over the $|\beta^-|$ moment, and the more positive the overall β_{xxx}. Reversing the argument, it is only for short chains that the $|\beta^-|$ polarization moment can be expected to exceed the $|\beta^+|$ charge moment.

We note that if one is interested in distinguishing the unit cell and chain-end contributions,[22–24] it is useful to split β_{xxx} into its contributions. From Fig. 10(b), it is seen that the b^- bond polarization terms become constant at the center of the molecule. Thus, multiplying this constant b^- by x^- gives the unit cell bond polarization moment b^-x^-. The total chain-end contribution to β^- is then obtained as the difference between the unit cell b^-x^- bond polarization moment multiplied by the number of bonds and the actual total β^- moment. In agreement with previous studies,[22] a ratio of -6 is obtained between the chain-end and individual unit cell contributions to β^-. For the β^+ moment, it is more difficult to extract the respective unit cell and chain-end contributions because, on the one hand, the values of b^+ at the center of the chain follow a linear behavior and, on the other hand, x^+ varies with the position of the bond.

In summary, the real-space analysis indicates that the negative bond polarization second-order nonlinearity β^- prevails in short PMI oligomers making the longitudinal hyperpolarizability negative, while the positive bond charge component β^+ dominates for longer oligomers. Loosely speaking, bond charge which corresponds to charge transfer over longer distances plays a more important role in longer chains than bond polarization which is limited to the charge transfer between two adjacent atoms. Therefore, bond charge nonlinearities ensure the positive second-order NLO response in long PMI chains. The more local character of the bond polarization contribution is consistent with early saturation of β^-/N with chain length, while β^+/N is not yet converged for $N=20$, as illustrated in Fig. 8. To cast these results in a more general perspective, it can be expected that static hyperpolarizability can be exclusively positive in extended conjugated systems, while negative values can be sought only for relatively short oligomers.

IV. CONCLUSIONS

The origin of the second-order polarizability of polymethineimine chains has been studied in the framework of the complementary SOS and real-space interpretation schemes.

In the SOS formalism, the interpretation of the NLO properties of a molecule is performed in terms of the electronic characteristics of the ground and excited states and of the couplings among them. By using a four-state model, which reproduces well the total SOS β_{xxx} value, we have shown that the sign of β_{xxx} is governed by the interplay between two contributions of opposite sign. Both of these change sign as N increases. In particular, the dipole moment of the first excited state changes sign with chain length, which accounts for the sign change of the two-state dipolar term in the SOS expression. However, as the chain length increases, many excited states enter the SOS expansion and a simple description of the nonlinearity is no longer possible.

In the real-space description of the charge polarization of the molecule, the molecular static second-order polarizability is expressed in terms of partitioned charges and of second-order bond charge and polarization moments. It is seen that the signs of the C=N bond polarization and charge moments are opposite; therefore, the sign of the molecular second-order polarizability is also resulting from a competition between two terms. In PMI, the bond charge nonlinearity corresponds to long-range charge transfers and leads to positive β_{xxx} values in long chains. The bond polarization nonlinear-

Downloaded 24 Sep 2003 to 138.48.16.177. Redistribution subject to AIP license or copyright, see http://ojps.aip.org/jcpo/jcpcr.jsp

ity is limited to the charge transfer between adjacent atoms; it is negative and dominates the second-order NLO response of short oligomers.

As a final remark we note that, unfortunately, it is difficult to relate in a direct way the descriptions of the NLO properties coming from the SOS and real-space FF methodologies. The reason is the following: the FF approach is variational; the wave functions of the molecule in the presence of an electric field are computed for each electric field value; since there is no simple analytical relationship among the wave functions at various fields, one has to calculate explicitly each wave function in order to extract the (hyper)polarizabilities. On the other hand, the SOS approach is perturbational, formulated in the one-electron basis of the HF MOs of the nonperturbed state, and its strength is that is does not require the complicated wave functions at different electric field values; a CI expansion is used in its context to obtain the (hyper)polarizabilties, expressed directly via the matrix elements over many-electron basis functions, i.e., determinants of nonperturbed MOs. Thus, the wave functions remain actually ignored, so does the electron density redistribution; in other words, the molecule's interaction with electric field is not characterized in real space.

ACKNOWLEDGMENTS

The Belgian National Fund for Scientific Research is gratefully acknowledged for a Post-Doctoral Researcher Assistant position to D.J., a Research Associate position to D.B., a Senior Research Associate position to B.C. and for the support of the scientific mission of J.M.A. at the University of Arizona. The authors thank partial support from FNRS–FRFC and Loterie Nationale (convention No. 2.4519.97); Belgian National Interuniversity Attraction Poles on Sciences of Interfacial and Mesoscopic Structures (PAI/IUAP No. P4/10), and Supramolecular Chemistry and Supramolecular Catalysis (PAI/IUAP No. P4/11); and U.S. National Science Foundation (CHE-0078819).

[1] D. Wöhrle, Tetrahedron Lett. **22**, 1969 (1971).
[2] D. Wöhrle, Makromol. Chem. **175**, 1751 (1974).
[3] M. H. Whangbo, R. Hoffmann, and R. B. Woodward, Proc. R. Soc. London, Ser. A **366**, 23 (1979).
[4] J. L. Brédas, B. Thémans, and J. M. André, J. Chem. Phys. **78**, 6137 (1983).
[5] J. Chandrasekhar and P. K. Das, J. Phys. Chem. **96**, 679 (1992).
[6] A. Karpfen, Chem. Phys. Lett. **64**, 299 (1979).
[7] A. K. Bakhshi and J. Ladik, Solid State Commun. **60**, 361 (1986).
[8] D. Jacquemin, B. Champagne, and J. M. André, J. Chem. Phys. **108**, 1023 (1998).
[9] M. Springborg, Ber. Bunsenges. Phys. Chem. **95**, 1238 (1991).
[10] M. Springborg, Z. Naturforsch., A: Phys. Sci. **48**, 159 (1993).
[11] S. Hirata and S. Iwata, J. Chem. Phys. **107**, 10 075 (1997).
[12] J. Q. Sun and R. J. Bartlett, J. Chem. Phys. **108**, 301 (1998).
[13] M. Kertesz, J. Koller, and A. Azman, Chem. Phys. Lett. **69**, 225 (1980).
[14] H. Teramae, T. Yamabe, and A. Imamura, J. Chem. Phys. **81**, 3564 (1984).
[15] I. D. L. Albert, P. K. Das, and S. Ramasesha, Chem. Phys. Lett. **176**, 217 (1991).
[16] T. Tsunekawa and K. Yamaguchi, Chem. Phys. Lett. **190**, 533 (1992).
[17] T. Tsunekawa and K. Yamaguchi, J. Phys. Chem. **96**, 10 268 (1992).
[18] D. Jacquemin, B. Champagne, and J. M. André, Synth. Met. **80**, 205 (1996).
[19] D. Jacquemin, B. Champagne, and J. M. André, J. Mol. Struct.: THEOCHEM **425**, 69 (1998).
[20] B. Champagne, D. Jacquemin, and J. M. André, Proc. SPIE **2527**, 71 (1995).
[21] D. Jacquemin, B. Champagne, J. M. André, and B. Kirtman, Chem. Phys. **213**, 217 (1996).
[22] B. Champagne, D. Jacquemin, J. M. André, and B. Kirtman, J. Phys. Chem. A **101**, 3158 (1997).
[23] D. Jacquemin, B. Champagne, and B. Kirtman, J. Chem. Phys. **107**, 5076 (1997).
[24] D. Jacquemin, B. Champagne, and J. M. André, Chem. Phys. Lett. **284**, 24 (1998).
[25] K. Schmidt and M. Springborg, Synth. Met. **85**, 1119 (1997).
[26] P. Otto, F. L. Gu, and J. Ladik, J. Chem. Phys. **110**, 2717 (1999).
[27] K. Schmidt and M. Springborg, Phys. Chem. Chem. Phys. **1**, 1743 (1999).
[28] F. Meyers, S. Marder, B. M. Pierce, and J. L. Brédas, J. Am. Chem. Soc. **116**, 10 703 (1994).
[29] D. Beljonne, F. Meyers, and J. L. Brédas, Synth. Met. **80**, 211 (1996).
[30] V. M. Geskin and J. L. Brédas, J. Chem. Phys. **109**, 6163 (1998).
[31] V. M. Geskin and J. L. Brédas, Synth. Met. **101**, 488 (1999).
[32] V. M. Geskin and J. L. Brédas, Synth. Met. **116**, 269 (2001).
[33] M. J. Frisch, G. W. Trucks, H. B. Schlegel *et al.*, GAUSSIAN 94, Revision B.1, Gaussian, Inc. (Carnegie-Mellon University, Pittsburg, PA, 1995).
[34] J. E. Ridley and M. Zerner, Theor. Chim. Acta **32**, 111 (1973).
[35] B. J. Orr and J. F. Ward, Mol. Phys. **20**, 513 (1971).
[36] P. Chopra, L. Carlacci, H. F. King, and P. N. Prasad, J. Phys. Chem. **93**, 7120 (1989).
[37] N. Nakano, I. Shigemoto, S. Yamada, and M. Yamaguchi, J. Chem. Phys. **103**, 4175 (1995).
[38] S. R. Marder, W. E. Torruellas, M. Blanchard-Desce, V. Ricci, G. I. Stegeman, S. Gilmour, J. L. Brédas, J. Li, G. U. Bublitz, and S. G. Boxer, Science **276**, 1233 (1997).
[39] Z. Shuai, D. Beljonne, and J. L. Brédas, J. Chem. Phys. **97**, 1132 (1992).

Downloaded 24 Sep 2003 to 138.48.16.177. Redistribution subject to AIP license or copyright, see http://ojps.aip.org/jcpo/jcpcr.jsp